IMPROVING AUTOMATED SEARCH FOR UNDERWATER THREATS USING MULTISTATIC SENSOR FIELDS BY INCORPORATING UNCONFIRMED TRACK INFORMATION

D. Angley, S. Mehrkanoon, B. Moran

School of Engineering,
The University of Melbourne,
Parkville, VIC 3010

C. Gilliam

School of Engineering,
RMIT University,
Melbourne, VIC 3000

S. Simakov

Maritime Division,
DSTG, Edinburgh,
SA 5111, Australia

ABSTRACT

Sonobuoy fields, comprising a network of sonar transmitters and receivers, are used to search for and track underwater targets. Although normally such fields are operated from a maritime patrol aircraft, automated scheduling and processing creates opportunities for employing them as autonomous sensor systems. The automated search mechanism considered in this work is controlled by modelling the presence of undetected threats in an Operational Area (OA) using a spatial probability density function (PDF), known as a threat map. The algorithm decides how to schedule waveform transmissions, known as pings, to efficiently search and clear the OA. A conventional approach is to update the threat map based on just the characteristics of the sonobuoy field and switch to a separate metric to track a target after track confirmation. In this study we address the phase when there are potential contacts which cannot yet be promoted to confirmed tracks. We develop a mechanism for probing the associated areas of interest while still remaining in the threat map driven search scheduling. To this end, we propose reinitialising the threat map after each transmission using an augmented PDF, where unconfirmed tracks are represented by weighted Gaussians. Simulations show that this approach significantly improves search performance, reducing the number of pings required to confirm a track, distance from a confirmed track to the target and the proportion of falsely confirmed tracks.

***Index Terms*—** Multi-static sonar, Sensor scheduling, Autonomous search.

1. INTRODUCTION

A sonobuoy is a compact deployable sonar system containing sonar transmitters and/or receivers that can be used to search for and track underwater targets. Multiple sonobuoys can be laid out in a sonobuoy field and be used cooperatively, with an operator or autonomous sensor management system deciding which sonobuoys should ping at any given time. The goal of the sonobuoy field is to search an Operational Area (OA) for an undetected threat; success is either the clearance of the area or the detection and accurate tracking of a target. In this paper, we focus on the search mode of operation. Once the presence of a target has been confirmed then the field switches to a tracking mode, where the focus is on high accuracy location and tracking of the target. A challenging aspect, however, is the confirmation of target; each transmission by the sonobuoy field results in many detections that may or may not relate to a target. To avoid false tracks, a track is confirmed once there is a high probability that the track is associated with a target. This confirmation process requires multiple detections to be associated across multiple pings, and hence coordination in the search mode to ensure detection opportunities. Accordingly, our focus is on optimising the search mode to reduce the number of pings (i.e. time) required to confirm a track and clear an area.

A threat map is used to model the spatial PDF of an existing, but undetected target [1–7]. This spatial PDF is updated as sonobuoys in the field transmit waveforms and process returns, lowering the probability that an undetected target could exist in areas near the transmitting sonobuoy according to the probability of detection. The PDF is also updated at each time step to take into account possible kinematics of the target. The threat map can be used as a planning tool, helping the operator to decide both where to place the sonobuoys and when each sonobuoy should transmit a waveform in order to effectively search an operational area. Section 2 details multiple approaches to calculating the threat map found in literature.

The existing methods of calculating a threat map are generally focused on modelling detections and detection probability, but in practice the decision to switch to tracking mode is based on more than just a single detection. The sonar environment is usually noisy and spurious detections are common. The system cannot switch to tracking mode for every detection, because this would waste time trying to track a target that does not exist while a true target continues to operate in another area. Detections are therefore processed by a tracker, which requires multiple consistent detections to confirm the presence of a target. Detections initially create unconfirmed tracks, with a low probability of being associated with a true target, and are either promoted to confirmed tracks or discarded based on subsequent detections.

In our previous work using threat maps to optimise sonobuoy search [8], we observed a mismatch between detecting and confirming a track, which could lead to suboptimal performance. A sonobuoy might ping and clear an area of the threat map, but if this was not followed up with subsequent pings in the same area then the tracker might discard the unconfirmed tracks by the time the area was revisited. In this paper we explore the impact of including the unconfirmed tracks from the tracker into the threat map in order to make more effective search decisions, such as repeatedly pinging in the same area in order to confirm or discard unconfirmed tracks. This is a novel approach that also has the advantage of being easy to retrofit to existing systems, taking advantage of their existing tracking algorithms. It moves application of the threat map from the planning of the mission to its execution, where additional information from detections can be used to schedule sonobuoy transmissions.

2. THREAT MAP

The threat map is a representation of the spatial PDF of an existing but undetected target. There are two main approaches in the literature for modelling undetected targets.

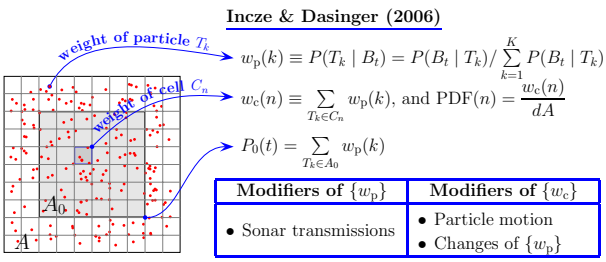

Fig. 1. The Incze & Dasinger [5, 6] approach to modelling the threat map. A large number of virtual targets (red dots) are distributed over area A. The particle weight (w_p) is calculated as the probability that the target is realised as virtual target k (event T_k) given that it hasn't been detected yet (event B_t), divided by the sum of probabilities for all K particles. The weight of a cell (w_c) is the sum the weights of all the particles within it, and the PDF of the target location is the cell weight divided by the cell area (dA). An area of interest (A_0) is shown, and the probability that the target is in that area (P_0) can be calculated by summing the weights of the particles it contains.

Krout et al. [1–4] model the probability of target presence using a regular grid of cells, and allow for target movement using a drift and diffusion model on this grid. The calculated parameter $P_{(i,j),k}$ is the probability of target presence in a cell (i, j) at step k, which is incremented at each time step or whenever the sonar transmission occurs. The amount by which a sonar transmission changes $P_{(i,j),k}$ depends on the probability of detection in the cell, while value $P_{(i,j),k+1}$ after the time step update is obtained using $P_{(s,q),k}$ from adjacent cells (s, q) by application of a 3×3 spatial Fokker-Planck (FP) filter which depends on the "drift" and "diffusion" coefficients associated with the considered target motion scenario. We used this technique in our previous work, which considered the tradeoff between tracking and search when scheduling transmissions in sonobuoy fields [8]. One of the limitations of the approach based on the FP filtering is that, for more complex scenarios, the translation of the target motion assumptions into drift and diffusion coefficients is not always straightforward. Using arbitrary values for these coefficients may produce an invalid filter. Some scenarios may require a higher-order finite-difference approximation and a larger size (5×5) of the FP filter. Note also that the fact that the probability of presence does not integrate to 1 implies that its transformation into a probability density function requires some form of rescaling. Such a rescaling procedure and an interpretation of its result are yet to be discussed in the published literature.

Incze and Dasinger [5, 6] call their model of the threat map a "Threat Density Probability Map". They use a Monte Carlo approach in which the target can be realised as one of the virtual targets from a large set of virtual targets initialised and propagated in accordance with the scenario of interest. The probability of target presence in an area given that it remains undetected as the sonobuoys transmit is calculated using Bayes's Theorem and a model of detection probability, as well as the target motion assumptions. This probability is normalised to sum to 1 over all target locations considered, modelling the assumption that a single target exists somewhere. Figure 1 details this approach.

The Incze and Dasinger method is computationally expensive because of the large number of virtual targets. However, Simakov and Fletcher [7] implement this model on the GPU, allowing for tens of thousands of virtual targets to be used. We use this approach to calculate the threat map in this paper, and Figure 2 shows an example of how this threat map evolves as sonobuoys ping.

A limitation of these approaches is that they do not take into account detection information available during operation. We now propose a method of incorporating this information into the threat map in order to reduce the number of pings required to confirm a target.

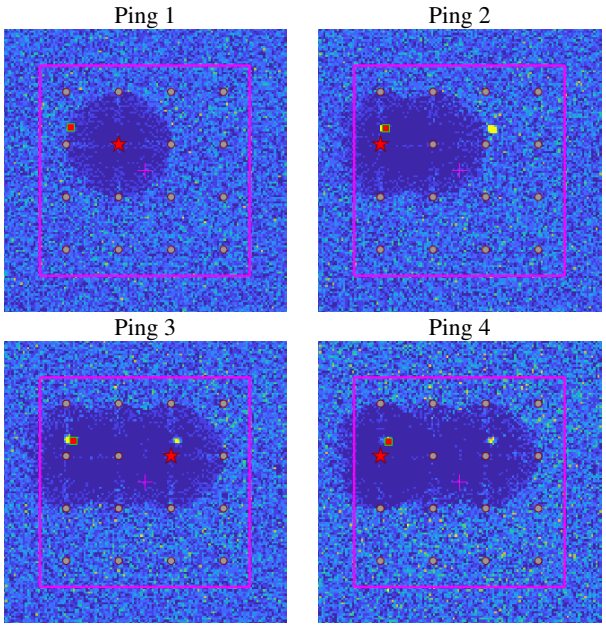

Fig. 2. Example showing how the threat map evolves as sonobuoys ping over four consecutive pings. The colour represents the probability density of target presence, with darker areas indicating lower probability. The sixteen grey circles show the sonobuoys, which are all both transmitters and receivers. The pink square shows the operational area which is being searched. The red square with a green outline shows the target location. The red star on a sonobuoy indicates that it has just emitted a waveform, which clears a roughly circular area around it by lowering the probability of target presence. The bright yellow blobs show unconfirmed tracks which have been incorporated into the threat map.

3. INCORPORATING UNCONFIRMED TRACKS INTO THE THREAT MAP

To overcome the limitations discussed previously, we now present our approach to incorporating unconfirmed target information into the threat map. For each sonar transmission, a small number of detections are received, which are used to update existing confirmed tracks or initiate a new unconfirmed track. The location $\mathbf{x}_k \equiv [x_k, y_k]^T$ and covariance matrix $\mathbf{C}_{xy}^k$ of each unconfirmed track ($k = 1, \ldots, K_t$), which are outputs from the tracker, were used to form the associated 2D Gaussian corrections to the evolving Threat Map PDF $p(\mathbf{x}, t)$

$$p(\mathbf{x}, t) \mapsto \gamma_0 p(\mathbf{x}, t) + \sum_{k=1}^{K_t} \gamma_k G(\mathbf{x} - \mathbf{x}_k; \mathbf{C}_{xy}^k) \qquad (1)$$

where

$$G(\mathbf{x}; \mathbf{C}_{xy}) \equiv \frac{\exp\left(-\frac{1}{2}\mathbf{x}^T \mathbf{C}_{xy}^{-1} \mathbf{x}\right)}{2\pi\sqrt{\det \mathbf{C}_{xy}}}$$

and $\sum_{k=0}^{K_t} \gamma_k = 1$. After each sonar transmission we first apply a standard threat map update [7], which accounts for ping-induced reduction of weights of virtual targets. In the simulations discussed in this paper, γ_k used in (1) had the following values: γ_0 fixed and $\gamma_k = (1 - \gamma_0)/K_t$ ($k > 0$).

Next we incorporate unconfirmed tracks into the resulting $p(\mathbf{x}, t)$ by adding weighted Gaussian corrections. This also uses

a reinitialisation procedure which produces a set of K_p equally-weighted particles $\{\mathbf{x}_\mathrm{p}(k),\ w_\mathrm{p}(k) = 1/K_\mathrm{p}\}$ spread over the cells of the threat map. Figure 3 illustrates calculation of the cell index for particle k. Here $U(0,1)$ is the uniform distribution in the interval $(0,1)$. We use the inversion method [9, Ch. 3]. The probability that a particle is placed into cell n is $w_\mathrm{c}(n)$, where the cell weights $\{w_\mathrm{c}(m)\}$ are obtained by integrating the post-ping PDF $p(\mathbf{x},t)$ in the respective cells. Once the cell for particle k has been identified, $\mathbf{x}_\mathrm{p}(k)$ is obtained by drawing from a uniform distribution defined in the cell. This process effectively imbues the threat map with a memory of all the previous detection information.

The repeated reinitialisation can result in clumping of particles into some cells at the expense of depopulation of the adjacent cells. Replacing pseudo-random generation used for production of $r_k \in U(0,1)$ during calculation of the particle cell index with a quasi-random approach (e.g. Sobol, or scrambled Sobol generators [10]) resolves this issue.

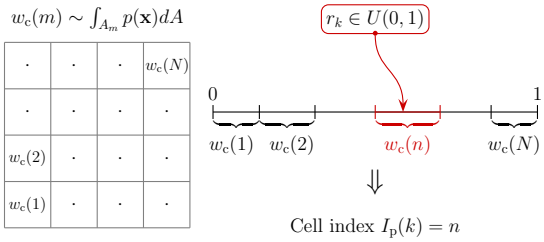

Fig. 3. Reinitialisation procedure: calculation of cell-index of particle k.

4. SCHEDULING MULTISTATIC SONOBUOY FIELDS

The key elements required to schedule a sonobuoy field are introduced here.

4.1. Sensor Scheduling Algorithm

Sensor scheduling in this sonobuoy scenario means choosing which sonobuoy to emit a waveform from in each ping interval T_p. In this paper we consider three scheduling algorithms: random, raster and lookahead scheduling. The random scheduler picks a uniformly random sonobuoy to transmit in each interval. The raster scheduler uses a predefined raster pattern of sonobuoys to ping from that loops until the target is found. The lookahead scheduler is a myopic scheduler that picks the sonobuoy that minimises the probability of target presence in the area of interest, A_0, after the next ping, as modelled by the threat map. Note, as discussed in the introduction, we only consider scheduling to optimise the search for an unknown target; the tracking and localisation of a confirmed target requires different optimisation criteria [8, 11].

We apply the lookahead scheduler to the threat map evolved in two different modes: conventional, as described by Figure 1, and our method of incorporating unconfirmed track information, as described in Section 3. Figure 4 shows a diagram of the simulation setup and summarises how the lookahead scheduler works when the latter mode is employed.

4.2. Measurement Simulation

We use the BRISE (Bistatic Range Independent Signal Excess) [12] simulation environment to simulate sonobuoy measurements. BRISE

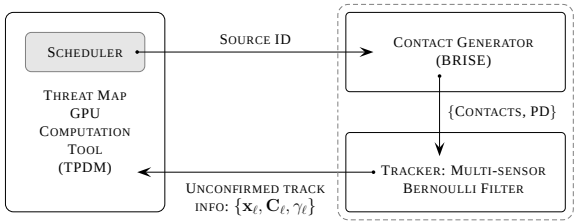

Adaptive (lookahead) ping selection workflow:

1. Before a transmission, probe different sources m to examine the difference between $p(\mathbf{x},t)$ and the post-ping $p_m(\mathbf{x})$
2. Select source ID s resulting in maximal reduction of the Probability of Presence P_0
3. Set post-ping PDF: $p(\mathbf{x},t) = p_s(\mathbf{x})$, where $s = \operatorname{indmax}_m \left(P_0[p(x,t)] - P_0[p_m(\mathbf{x})]\right)$
4. Contact generator uses the actual target(s) and the source ID s to generate contacts
5. The tracker uses the contacts and the source ID s to produce $\{\mathbf{x}_\ell, \mathbf{C}_\ell, \gamma_\ell\}$
6. Update post-ping PDF: $p(\mathbf{x},t) \to \gamma_0 p(\mathbf{x},t) + \sum_{\ell=1}^{L} \gamma_\ell G_\ell(\mathbf{x} - \mathbf{x}_\ell; \mathbf{C}_\ell)$
7. Propagate virtual targets and evolve $p(\mathbf{x},t)$ up to the time of the next transmission

Fig. 4. Simulator setup, showing interaction between the threat map GPU computation tool, the contact generator, and the tracker in the case when the lookahead scheduler is applied to a threat map augmented by unconfirmed tracks.

uses lookup tables containing signal excess data, precomputed using the Gaussian ray bundle eigenray propagation model [13], to calculate a signal-to-noise ratio (SNR) for each target and produce measurements of the bistatic range and bearing, along with false alarms [14]. The simulations in this paper all use a linear frequency modulation (LFM) waveform centred at 2 kHz with a transmission duration of 2 seconds and bandwidth of 200 Hz.

4.3. Tracker

In order to provide unconfirmed tracks to combine with the threat map, we use a multi-target tracking algorithm [14, 15] that has been extensively evaluated for tracking targets in similar sonobuoy scenarios [8, 11, 16, 17] and found to perform robustly. The tracker uses the multi-sensor Bernoulli filter [18, 19], the optimal Bayesian multi-sensor filter for a single target, and applies the linear-multitarget paradigm [20] to extend it to track multiple targets. In particular, we use the Gaussian mixture model implementation of this algorithm. The tracker estimates a probability of target existence for each track, along with a track status that indicates if the track is confirmed (i.e. high probability of being associated with a true target) or unconfirmed.

5. RESULTS

In order to evaluate the performance of the system shown in Figure 4 and demonstrate the advantage of using unconfirmed track information in the threat map, we used simulations of the scenario shown in Figure 5. This scenario has 16 sonobuoys, arranged in a 4×4 grid and spaced 20 km apart. In each simulation, the target starts at a random position uniformly distributed in the 5 km neighbourhood of the boundary of the operational area and moves towards the centre of the field. The scenario is run until the tracker reports its first confirmed track, at which point the field would switch modes from search to tracking in a practical scenario. The performance metrics gathered are the number of pings until the track is confirmed, the proportion of falsely confirmed tracks, and the distance between the target location and the confirmed track. A falsely confirmed track is

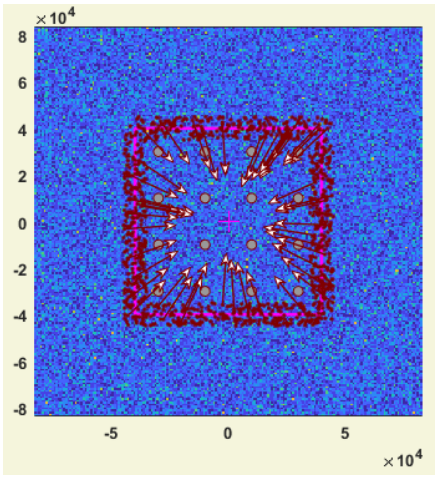

Fig. 5. Sonobuoy scenario, with 16 sonobuoys (grey circles) laid out in a grid spaced 20 km apart. The red dots show sample target trajectories, starting in the neighbourhood of the boundary of the operational area and moving towards the centre. The pink square shows A_0, the area of interest, which is a square area from $(-40, -40)$ km to $(40, 40)$ km.

defined as a confirmed track position estimate that is more than 1 km from the true target position, and these are excluded from the mean distance calculation.

Simulations were performed for the four different scheduling methods detailed in Section 4.1, which are labelled Raster (predefined sweeping pattern), Random (uniform random selection of sonobuoy), Lookahead (lookahead scheduling without incorporating unconfirmed tracks) and Unconfirmed (lookahead scheduling incorporating unconfirmed tracks). 1,000 Monte-Carlo simulations were performed for all methods and for various values of γ_0.

Figure 6 shows the results from these simulations. The three methods that do not use unconfirmed track information all show similar performance on the number of pings to confirm a track, taking a mean of 24.9 to 26 pings to confirm a track. Incorporating unconfirmed track information into the threat map reduced this number of pings significantly, down to 13.5 pings for $\gamma_0 = 0.93$. Importantly, the corresponding proportion of falsely confirmed tracks is also lower for the Unconfirmed method. Thus, the improvement in confirmation is due to the tracker confirming true tracks faster not false tracks. The mean distance between the target and the confirmed track at confirmation time was also lower for the Unconfirmed method, indicating that this method also improves track error at confirmation time. The performance of the Unconfirmed method was fairly stable across a wide range of γ_0 and converges with the performance of the Lookahead method as γ_0 approaches 1 as expected, because no unconfirmed track information is incorporated when $\gamma_0 = 1$.

Figure 7 shows 2D histograms of the proportion of pings emitted from each sonobuoy, with a layout matching Figure 2. Raster shows the characteristic vertical scanning pattern, from the bottom left to the top right. Random is uniformly distributed, as expected. Lookahead shows unbalanced usage of the field, focusing on the edges and corners once the centre of the field has been cleared because that is where a target will likely enter from. By contrast, Unconfirmed shows more balanced sonobuoy usage which is somewhere between Lookahead and Random, with a focus on the edges of the field but the unconfirmed tracks leading it to make greater usage of the other sonobuoys.

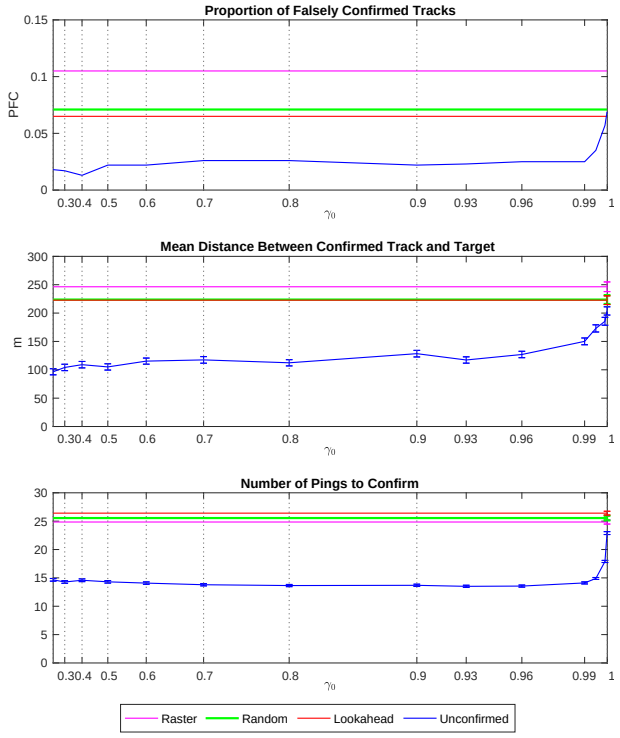

Fig. 6. Simulation results, showing the proportion of falsely confirmed tracks, mean distance between the confirmed track and the true target and the number of pings to confirm a target for the 4 methods. Performance is shown for a range of γ_0 values, with Unconfirmed being the only method that depends on this parameter. The error bars show plus or minus one standard deviation.

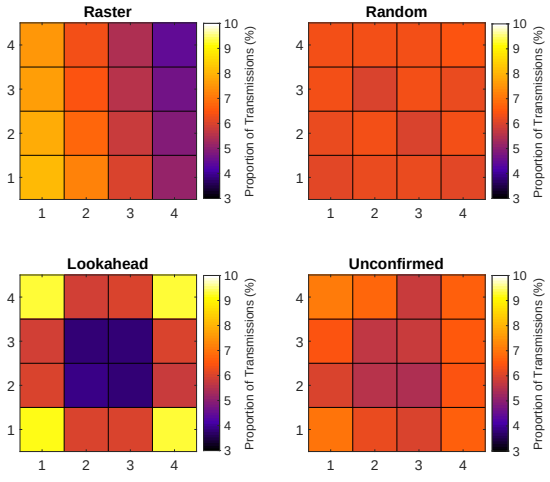

Fig. 7. 2D histogram of the proportion of pings transmitted by each sonobuoy of the 4×4 field in simulations of the four different scheduling methods.

6. CONCLUSION

In this paper we have presented a novel approach to improving autonomous search of an area of interest using a sonobuoy field. By incorporating unconfirmed track information from the tracker into the threat map, we demonstrate a significant increase in performance, reducing the number of transmissions required to confirm the presence of an underwater threat, such as a submarine or a sizeable UUV.

The confirmed tracks were also more accurate and there was a lower proportion of falsely confirmed tracks. This suggests that utilising the proposed technique in the search mode of multistatic systems could be valuable in practice, and our approach can take advantage of the existing tracking algorithms of such systems. Future work includes exploring alternative ways of combining unconfirmed tracks with the threat map.

7. REFERENCES

[1] D. W. Krout, M. A. El-Sharkawi, W. L. Fox, and M. U. Hazen, "Intelligent ping sequencing for multistatic sonar systems," in *Proceedings of the 9th International Conference on Information Fusion*. IEEE, 2006, pp. 1–6.

[2] D. W. Krout, W. L. Fox, and M. A. El-Sharkawi, "Probability of target presence for multistatic sonar ping sequencing," *Oceanic Engineering, IEEE Journal of*, vol. 34, no. 4, pp. 603–609, 2009.

[3] D. W. Krout, G. M. Anderson, E. Hanusa, and B. D. Jones, "Threat modeling for sensor optimization," in *2013 OCEANS-San Diego*. IEEE, 2013, pp. 1–4.

[4] D. W. Krout and T. Powers, "Sensor management for multistatics," in *17th International Conference on Information Fusion (FUSION)*. IEEE, 2014, pp. 1–6.

[5] B. I. Incze and S. B. Dasinger, "Revisiting measures of effectiveness in support of low-frequency, multistatic sonar search in the littoral battlespaces," Tech. Rep., Naval Undersea Warfare Center, Newport RI, 2000.

[6] B. I. Incze and S. B. Dasinger, "A bayesian method for managing uncertainties relating to distributed multistatic sensor search," in *Proceedings of the 9th International Conference on Information Fusion*. IEEE, 2006, pp. 1–7.

[7] S. Simakov and F. Fletcher, "GPU acceleration of threat map computation and application to selection of sonar field controls," in *IEEE International Conference on Acoustics, Speech and Signal Processing (ICASSP)*. IEEE, 2015, pp. 1827–1831.

[8] C. Gilliam, B. Ristic, D. Angley, S. Suvorova, B. Moran, F. Fletcher, H. Gaetjens, and S. Simakov, "Scheduling of multistatic sonobuoy fields using multi-objective optimization," in *2018 IEEE International Conference on Acoustics, Speech and Signal Processing (ICASSP)*. IEEE, 2018, pp. 3206–3210.

[9] L. Devroye, *Non-Uniform Random Variate Generation*, Springer-Verlag, 1986.

[10] "cuRAND Library: Programming Guide," NVIDIA, PG–05328–050, July 2019, https://docs.nvidia.com/cuda/.

[11] C. Gilliam, D. Angley, S. Williams, B. Ristic, B. Moran, F. Fletcher, and S. Simakov, "Covariance cost functions for scheduling multistatic sonobuoy fields," in *2018 21st International Conference on Information Fusion (FUSION)*. IEEE, 2018, pp. 1–8.

[12] S. Simakov, "Signal excess data and tools for multistatic sonar emulation," Tech. Report DSTO-TR-3026, DSTO, 2014.

[13] H. Weinberg and R. E. Keenan, "Gaussian ray bundles for modeling high-frequency propagation loss under shallow-water conditions," *The Journal of the Acoustical Society of America*, vol. 100, no. 3, pp. 1421–1431, 1996.

[14] B. Ristic, D. Angley, F. Fletcher, S. Simakov, H. Gaetjens, S. Suvorova, and B. Moran, "Bayesian multitarget tracker for multistatic sonobuoy systems," in *Proceedings of the 19th International Conference on Information Fusion*. IEEE, 2016, pp. 2171–2178.

[15] B. Ristic, D. Angley, S. Suvorova, B. Moran, F. Fletcher, H. Gaetjens, and S. Simakov, "Gaussian mixture multitarget–multisensor Bernoulli tracker for multistatic sonobuoy fields," *IET Radar, Sonar & Navigation*, vol. 11, no. 12, pp. 1790–1797, 2017.

[16] D. Angley, B. Ristic, S. Suvorova, B. Moran, F. Fletcher, H. Gaetjens, and S. Simakov, "Non-myopic sensor scheduling for multistatic sonobuoy fields," *IET Radar, Sonar & Navigation*, vol. 11, no. 12, pp. 1770–1775, 2017.

[17] D. Angley, S. Suvorova, B. Ristic, W. Moran, F. Fletcher, H. Gaetjens, and S. Simakov, "Sensor scheduling for target tracking in large multistatic sonobuoy fields," in *2017 IEEE International Conference on Acoustics, Speech and Signal Processing (ICASSP)*. IEEE, 2017, pp. 3146–3150.

[18] B.-T. Vo, C.-M. See, N. Ma, and W. T. Ng, "Multi-sensor joint detection and tracking with the Bernoulli filter," *IEEE Trans. Aerospace and Electronic Systems*, 2012.

[19] B. Ristic and A. Farina, "Target tracking via multi-static doppler shifts," *IET Radar, Sonar & Navigation*, vol. 7, no. 5, pp. 508–516, 2013.

[20] D. Musicki and B. La Scala, "Multi-target tracking in clutter without measurement assignment," *IEEE Trans. Aerospace and Electronic Systems*, vol. 44, no. 3, pp. 877–896, July 2008.